

Characterization of a 10-MHz quadrant APD for measuring frequency oscillations and tip displacements of microcantilevers

Brian G. Burke · David A. LaVan

Received: 3 November 2011 / Revised: 6 March 2012 / Published online: 16 September 2012
© Springer 2012

Abstract The room-temperature response of a 10-MHz quadrant avalanche photodiode (APD) is investigated for detection of high frequency oscillations and tip displacements of fabricated microcantilevers. Currently, no quadrant detectors with a response bandwidth in the megahertz range are available, and oscillations on the order of a few microseconds cannot be resolved. A comparison is made between optical and opto-mechanical measurements to characterize this detector by investigating the frequency response and signal-to-noise (SNR) of pulsed laser signals up to 10 MHz and reflected laser signals from freely vibrating microcantilevers up to 1.64 MHz. The power level of the minimum detectable signal incident on the APD is found to be 28.2 ± 5.0 nW for optical measurements and $1.0 \mu\text{W} \pm 5.0$ nW for opto-mechanical measurements.

1 Introduction

Avalanche photodiodes (APDs) have been used for various applications, including atomic force microscopy (AFM) [1], Raman spectroscopy [2], position sensing [3], laser tracking systems [4, 5], and scintillation detection [6, 7]. Particularly, quadrant APDs allow tip deflections and resonant frequency shifts of cantilevers to be measured with high precision using heterodyne techniques, which have been utilized in scanning probe microscopy (SPM) [8–13] and thermogravimetric analysis (TGA) [14–17]. Due to

significant advances in the development of high bandwidth quadrant APDs, research interests have focused on the characterization methods for these higher frequency devices [4, 5, 18].

Incident power levels exceeding 1.0 mW on cantilevers have caused deviations in the resonant frequencies [11], which is detrimental to TGA and SPM, and led to the development of more sensitive modules capable of operating under low power conditions, typically less than $10.0 \mu\text{W}$. Additionally, microcantilevers with resonant frequencies in the megahertz range have faster response times than traditional AFM cantilevers, which allows for faster scanning rates in SPM and quicker thermal response in TGA. However, the smaller microcantilever geometries require even smaller laser spot sizes, on the order of a few microns, which are achieved only with high numerical aperture (NA) focusing optics.

A nominally 12 MHz quadrant APD detection module was tested with an active receiving area of four independent cells in a 2×2 array. Each cell has an active area of 4 mm^2 and a $50\text{-}\mu\text{m}$ transition region between adjacent cells, and the instrument provides four independent voltage output signals, one per cell. The accompanying power supply operates in a variable reverse bias mode from 512 to 2,000 V. The quantum efficiency, as supplied by the manufacturer, is 75 % in the range of 830–905 nm, and 68 % in the range of 630–640 nm (Radiation Monitoring Devices (RMD), 44 Hunt Street, Watertown, MA 02472, USA). Visible laser light (630–640 nm) was used in the following experiments in order to clearly focus the laser spot onto the microcantilever tip. The unit was designed to operate from DC to 12 MHz with an ideal modulation range from 10 kHz to 5 MHz (Radiation Monitoring Devices (RMD), 44 Hunt Street, Watertown, MA 02472, USA).

B. G. Burke · D. A. LaVan (✉)
Ceramics Division, Material Measurement Laboratory, National
Institute of Standards and Technology, Gaithersburg,
MD 20899, USA
e-mail: david.lavan@nist.gov

In this work, the optical performance of the quadrant APD under low power illumination of 50 nW–1.0 μ W and frequency source modulation of 100 Hz–10 MHz was evaluated and compared to the response measured using opto-mechanically detected freely vibrating microcantilevers. We demonstrate that the quadrant APD, operated in differential or split detection mode, can be used in conjunction with high NA objectives to detect small tip oscillations of microcantilevers in the megahertz range.

2 Experimental setups

Two different experimental setups were used to evaluate and compare the response of the quadrant APD. Figure 1 shows the schematic of the experimental setups: (a) optical measurement and (b) opto-mechanical measurement. The optical measurement consists of a beam from a pulsed diode laser (PicoQuant, PDL 800-B, 2.0 mW), which is collimated and passed through two apertures, to precisely define the spot size, and directed onto the APD (Fig. 1a). The spot size can be adjusted and the APD is translated to measure the voltage response for individual cells and between adjacent cells. The pulsed diode laser can be operated from 100 Hz to 20 MHz and has a pulse-height standard deviation of 0.6 % (mean = 633.7 mV, std. dev. = 3.68 mV, $n = 20$).

The opto-mechanical measurement consists of a beam from a CW HeNe laser (Melles-Griot, 05-LHR-151, 10.0 mW), which is linearly and circularly polarized, to

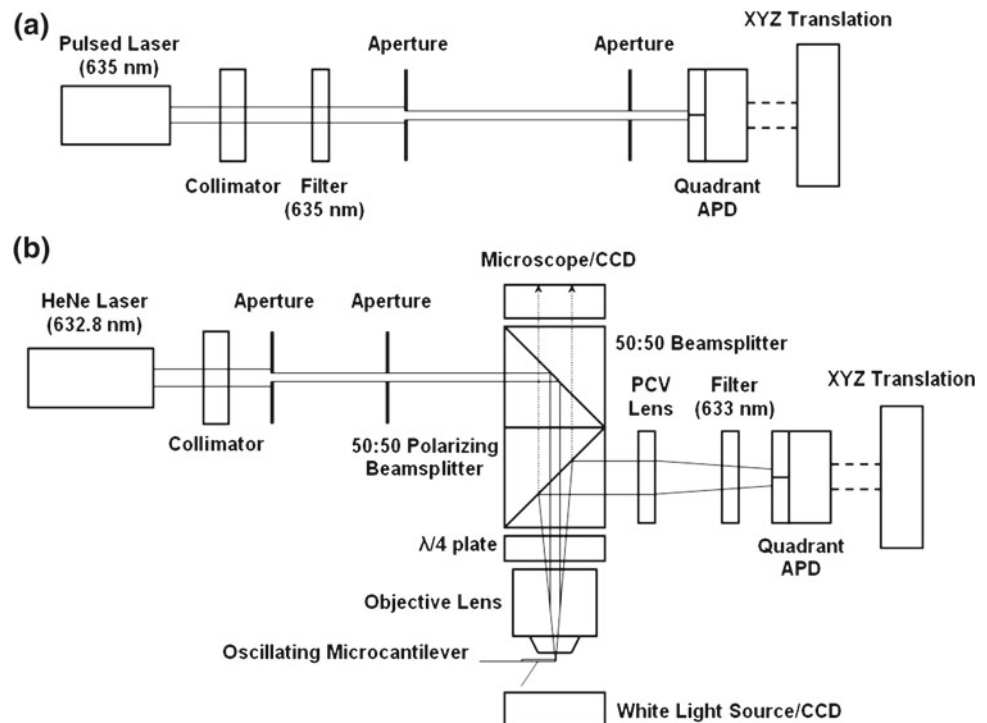
allow reflected signals off a microcantilever to be separated and focused onto the APD (Fig. 1b). The quadrant APD is operated in differential or split detection mode, in order to detect small tip deflections of microcantilevers. An infinity-corrected objective (Olympus, UPlanFL N, 20X/NA0.50) allows the viewing system to be confocal with the incident beam and produces a spot size of 4.0 μ m. This setup is necessary for detecting microcantilevers, for which the focus is more critical than for large commercial cantilevers. In addition, the incident beam is normal to the plane of the microcantilever, which minimizes the amount of laser light lost from shadowing, allows for precise focusing of the spot onto the microcantilever tip, and allows the reflected beam to be collected through the same focusing objective and finally separated by the polarizing beamsplitter.

Microcantilever samples were fabricated atop of a 100-mm Si(100) wafer using standard nanofabrication and etching methods. All microcantilevers were thermally self-activated and no external driving force was applied. The microcantilever acts as a transducer, converting heat energy in the environment to mechanical energy. The thermo-mechanical signal can be measured once the microcantilever has entered a steady state.

3 Results and discussion

The quadrant APD was evaluated with pulsed laser spots and reflected laser spots from oscillating microcantilevers.

Fig. 1 Schematic of the experimental setups: **a** optical measurement and **b** opto-mechanical measurement. The optical measurement consists of a beam from a pulsed diode laser, which is collimated and passed through two apertures, to precisely define the spot size, and directed onto the APD. The spot size can be adjusted and the APD is translated to measure the voltage response for individual cells and between adjacent cells. The opto-mechanical measurement consists of a beam from a HeNe laser, which is linearly and circularly polarized, to allow the reflected signal off a microcantilever to be separated and focused onto the APD. The quadrant APD is operated in differential or split detection mode, in order to detect small tip deflections of microcantilevers



When incorporated in the optical experimental setup (Fig. 1a), the voltage gain, voltage SNR, sensitivity (mV/ μm), and frequency response of individual cells can be measured. When utilized in the opto-mechanical experimental setup (Fig. 1b), which is similar to common SPM setups [9, 11], the quadrant APD can be evaluated to determine if the differential voltage mode has high enough sensitivity, SNR, and bandwidth to detect small tip deflections of microcantilevers oscillating in the megahertz range.

3.1 Optical measurement

Measurements were conducted at STP with the pulsed diode laser (635 nm illumination) operated from 100 Hz to 10 MHz. Each APD has a different breakdown and onset voltage. The voltage amplitude signal for each cell was measured as a function of the reverse bias voltage, and the results were normalized by the voltage signal at the initial onset reverse bias voltage to calculate the voltage gain. The voltage gain for a 1.0 mm spot at 50 nW centered on each cell as a function of the reverse bias voltage is shown in Fig. 2. The maximum voltage gain is 1,613. The voltage gain variation between the different quadrants is within 7.5 % for gains less than 1,300, and 16.7 % for the highest gains. Signals in all quadrants saturate at the breakdown voltage at 1,900 V.

The voltage SNR was measured in the center of cell A as a function of optical power with a reverse bias of

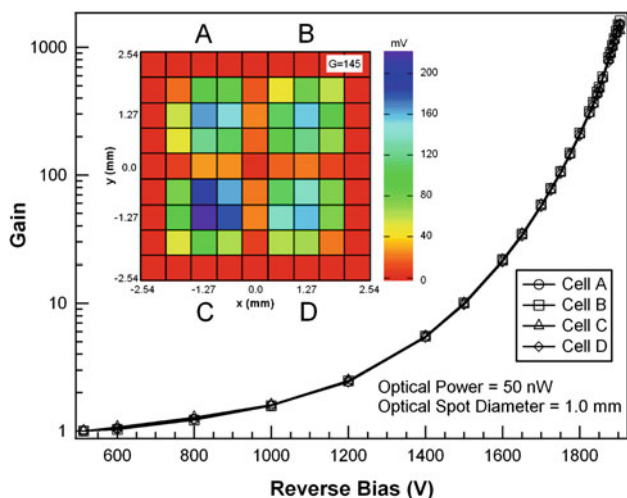


Fig. 2 The voltage gain for each cell, laser light positioned at the center of each cell, as a function of the reverse bias voltage for 635 nm illumination and 200 ns pulse duration. The maximum voltage gain is 1,613. The voltage gain variation between the different quadrants is within 7.5 % for gains less than 1,300, and 16.7 % for the highest gains. *Inset* identifies each cell and shows a 2D map (9 × 9 array) of the quadrant APD response, indicating active, inactive, and transition regions. The response was measured with 50 nW laser light, 1,775 V reverse bias, and a spot size of 0.65 mm, corresponding to a voltage gain of 145 (*color online*)

1,775 V, corresponding to a voltage gain of 145 (Table 1). The voltage SNR increases as the optical power increases. A linear fit of the data gives 0.184 SNR/nW \pm 0.02 SNR/nW (slope = 0.184 SNR/nW, std. dev. = 0.02 SNR/nW, $n = 4$). A 2D map of the voltage response for the quadrant APD with a 0.65 mm spot at 50 nW is shown in Fig. 2 (inset). A stationary beam was scanned on a 9 × 9 array, covering a 5.08 × 5.08 mm area, by translating the APD to characterize the response. Due to the fact that the chip has transition regions and that the light spot is circular, some sub-regions could not be completely evaluated. The standard deviation at the centers of the individual cells is 17.6 mV (mean = 173 mV, std. dev. = 17.6 mV, $n = 4$), while the standard deviation for the entire active areas of the quadrants is 8.33 mV (mean = 104.5 mV, std. dev. = 8.33 mV, $n = 36$). The 2D map of the voltage response indicates that the optical response is maximized at the center of each cell, and that the response may decrease if the quadrant APD is used in differential or split detection mode. This is due to the decreased voltage response near the transition regions between adjacent cells and greatly depends on the laser spot size and input power.

The sensitivity (mV/ μm) between cells A and B for different optical spot diameters at 50 nW is shown in Fig. 3. The sensitivity is a measure of the APD voltage response to a known translation. This measurement through the centers of cells A and B determines the optimum spot size, indicates that the size of the laser spot should be adjusted to maximize the response, and can be used to measure the position of a light-emitter. The sensitivity can be used to determine the positions of a microcantilever tip, and therefore, the tip displacement. The sensitivity increases as the optical spot diameter approaches 1.0 mm. A linear fit applied to the active region in cell A, over a range of 500 μm at 1,880 V reverse bias, gives 4.58 mV/ μm for a 1.0 mm spot, and 3.05 mV/ μm and 3.04 mV/ μm for 0.5 mm and 1.5 mm spots, respectively. For a 1.0-mm spot, the optimum center position is shown in Fig. 3 to be 400 μm away from the transition region, the point of steepest descent.

Frequency dependence of measurements in the range of 100 Hz–10 MHz was conducted on the quadrant APD

Table 1 The voltage SNR was measured in the center of cell A for different optical powers at 1,775 V, corresponding to a voltage gain of 145. The voltage SNR increases as the optical power increases. A linear fit of the data gives 0.184 SNR/nW \pm 0.02 SNR/nW (slope = 0.184 SNR/nW, std. dev. = 0.02 SNR/nW, $n = 4$)

Power (nW)	SNR (V/V)
28.2	5.0
50.0	10.2
100.0	16.5
200.0	37.2

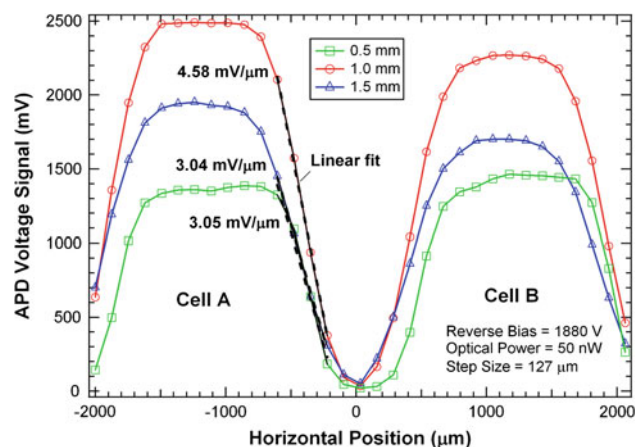


Fig. 3 Optical measurement of the sensitivity ($\text{mV}/\mu\text{m}$) through the centers of cells A and B for different optical spot diameters for 635 nm illumination and 200 ns pulse duration at 50 nW and 1,880 V reverse bias. A linear fit (dotted line) applied over a range of 500 μm determined a sensitivity of 4.58 $\text{mV}/\mu\text{m}$ for a 1.0 mm spot. Sensitivities of 3.05 $\text{mV}/\mu\text{m}$ and 3.04 $\text{mV}/\mu\text{m}$ were measured for 0.5 mm and 1.5 mm spots, respectively (color online)

under this optimal condition (Fig. 4). A decaying exponential fit of the optical measurement indicates the overall trend of the frequency response. The voltage SNR decreases as the laser light enters into the megahertz range and cannot be detected above 10 MHz. The voltage SNRs for frequencies in the range of 1–10 MHz vary from 23 to 6 as the frequency increases, which is still above the Rose criterion.

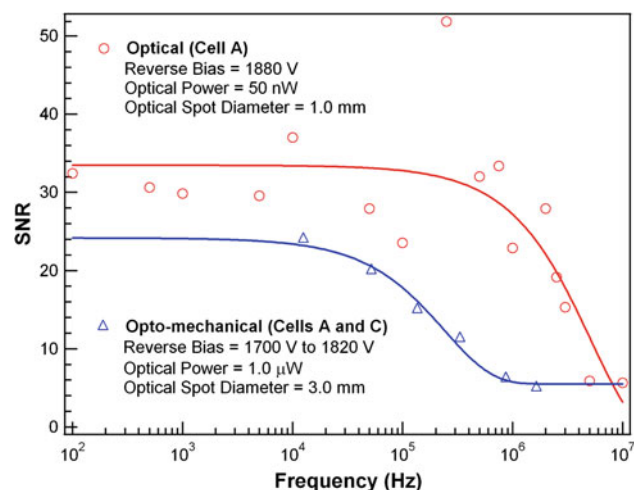


Fig. 4 Frequency dependence of measurements in the range of 100 Hz–10 MHz conducted on the quadrant APD to compare optical and opto-mechanical measurements. The optical measurement utilized a single cell (A) with a pulsed (635 nm illumination) source. The opto-mechanical measurement utilized a CW HeNe (632.8 nm illumination) source and acquired the thermo-mechanical signal of freely vibrating microcantilevers by measuring the RMS differential voltage between two cells (A–C). The decaying exponential fits (solid lines) indicate the overall trend of the frequency response (color online)

3.2 Opto-mechanical measurement

Quadrant detectors will often be used to detect cantilever motion. Thus, a comparison between optical and opto-mechanical measurements is critical for optimizing the experimental setup to detect small tip oscillations of microcantilevers in the megahertz range. In order to accomplish this, a differential opto-mechanical measurement must be conducted [9–13], where the APD is operated in differential voltage or split detection mode. The thermo-mechanical noise spectrum of freely vibrating microcantilevers was acquired by measuring the differential voltage between two adjacent cells.

The microcantilevers were thermally self-activated, and detected by the CW HeNe laser (632.8 nm illumination) at a minimum power of 10.0 μW and spot size of 4.0 μm . The sensitivity ($\text{mV}/\mu\text{m}$) depends on the beam power and beam spot size on the APD. At 50 nW and 1.0 mm spot size, no amplitude signal could be detected in the uncorrelated white noise. As the beam power increased, an amplitude peak in the frequency spectrum was detected. The spot size on the APD was adjusted in conjunction with the power, and an optimized signal occurred at a beam size of 3.0 mm and beam power of 1.0 μW . Discrete opto-mechanical frequency and SNR measurements are shown in Fig. 4.

The opto-mechanical SNR is lower and degrades at a lower frequency than that of the optical measurement, despite the increased sensitivity (8.81 $\text{mV}/\mu\text{m}$) due to the beam power increase. Additionally, the opto-mechanical signal is maximized when the beam size on the APD is 3.0 mm, allowing the centers of cells A and C to collect the reflected signal. These results indicate that the maximum response is at the center of each cell and a differential or split detection mode measurement is limited by the beam spot size.

Despite the decrease in SNR, the opto-mechanical measurement indicates that, at the appropriate beam power and beam spot size, the quadrant APD can detect microcantilever oscillations in the megahertz range. The quadrant APD acquired the RMS voltage signal of the undriven fabricated microcantilevers by measuring the differential voltage between two cells, (A–C), to detect the motion of the flexural vibration mode (Fig. 5). Lorentzian fits (solid lines) were applied to the thermo-mechanical signal and uncorrelated white noise. Additionally, the response of two commercially available Au-coated Si_3N_4 V-shaped cantilevers (Veeco, DNP, “C” and “D”), with larger surface areas and lower resonant frequencies, was measured to check the frequency response in the kilohertz range. The numerical results of resonant frequencies and SNRs for the different microcantilever geometries are listed in Table 2. The quality factors, measured in air, of all microcantilevers ranged from 22 to 30.

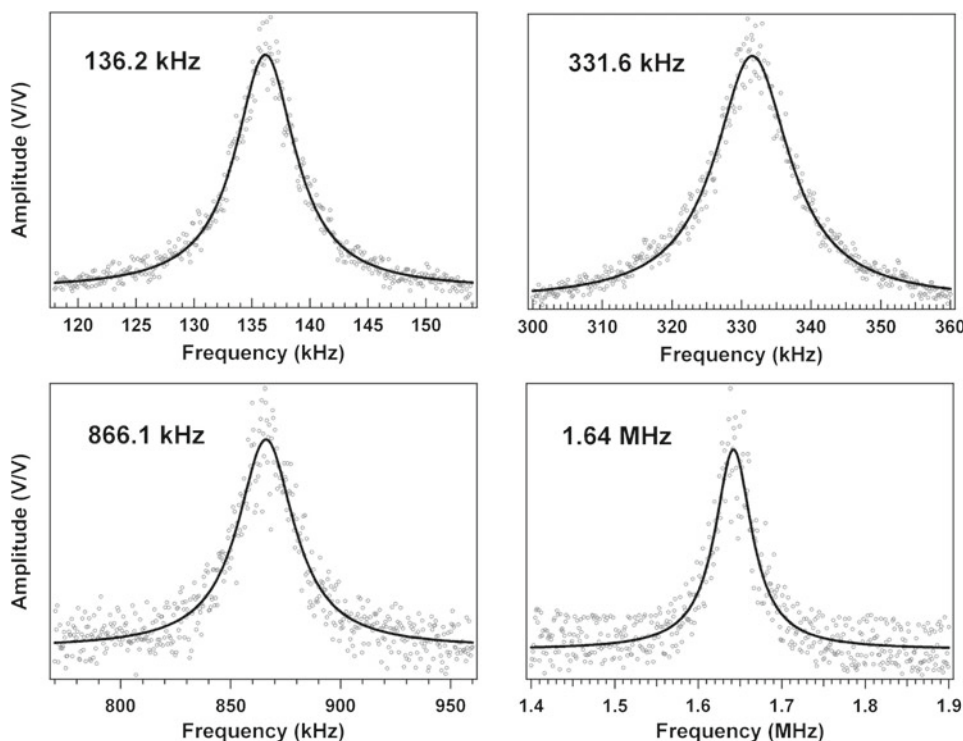


Fig. 5 Opto-mechanical measurements of the thermo-mechanical noise spectrum of freely vibrating microcantilevers. The quadrant APD acquired the RMS voltage signal of the undriven microcantilevers by measuring the differential voltage between two cells, (A–C), to detect the motion of the flexural vibration mode. The amplitude (V/V) plotted is the differential voltage amplitude, which is normalized

Table 2 The quadrant APD acquired the RMS voltage signal of undriven fabricated and commercially available microcantilevers by measuring the differential voltage between two cells, (A–C), to detect the motion of the flexural vibration mode

Microcantilever (μm)	Frequency (kHz)	SNR (V/V)
25×200	12.5	24.0
20×110	52.0	20.0
4×20	136.2	15.0
2×10	331.6	11.3
1×5	866.1	6.2
1×5	1,640.0	5.0

Lorentzian fits were applied to the thermo-mechanical signal to determine the resonant frequency and SNR

4 Conclusions

We have characterized a 10-MHz quadrant avalanche photodiode and detected frequency oscillations and tip displacements of microcantilevers. A comparison of the frequency response, SNR, and sensitivity ($\text{mV}/\mu\text{m}$) is made between optical and opto-mechanical measurements. We demonstrate that the quadrant APD, operated in differential or split detection mode, can be used in conjunction with

by the peak amplitude of each cantilever. The microcantilevers were thermally self-activated, and detected by a CW HeNe (632.8 nm illumination) at a minimum power of $10.0 \mu\text{W}$ and a spot size of $4.0 \mu\text{m}$. The reflected light on the APD was detected at $1.0 \mu\text{W}$ with an optical spot of 3.0mm . The *solid black lines* are Lorentzian fits to the thermo-mechanical signal and uncorrelated white noise

high NA objectives to detect small tip oscillations of microcantilevers in the megahertz range. We have confirmed the frequency response of pulsed laser signals up to 10 MHz and reflected laser signals from freely vibrating microcantilevers up to 1.64 MHz. The power level of the minimum detectable signal incident on the APD is found to be $28.2 \pm 5.0 \text{ nW}$ for optical measurements and $1.0 \mu\text{W} \pm 5.0 \text{ nW}$ for opto-mechanical measurements.

The opto-mechanical SNR is lower and degrades at a lower frequency than that of the optical measurement. The opto-mechanical signal is maximized when the beam size on the APD is 3.0mm , allowing the centers of cells A and C to collect the reflected signal. At the appropriate beam power and beam spot size, the quadrant APD operating in differential or split detection mode can detect microcantilever oscillations in the megahertz range.

Scanning probe microscopy (SPM) and thermogravimetric analysis (TGA) can utilize quadrant APDs to measure tip deflections and resonant frequency shifts. Efforts to improve scanning rates and response times for SPM and TGA require smaller cantilevers, lower illumination levels, and detectors with higher bandwidths. These measurements demonstrate the relationship between SNR and frequency response for optical and opto-mechanical measurements

incorporating new, high bandwidth quadrant APDs for next generation SPM and TGA.

Research is performed in part at the NIST Center for Nanoscale Science and Technology. Certain commercial equipment, instruments, or materials are identified in this document. Such identification does not imply recommendation or endorsement by the National Institute of Standards and Technology, nor does it imply that the products identified are necessarily the best available for the purpose.

References

1. M. Pierce, J. Stuart, A. Pungor, P. Dryden, V. Hlady, *Langmuir* **10**, 3217 (1994)
2. L.G. Cancado, A. Hartschuh, L. Novotny, *J. Raman Spectrosc.* **40**, 1420 (2009)
3. K.S. Shah, R. Grazioso, R. Farrell, J. Glodo, M. McClish, G. Entine, P. Dokhale, S.R. Cherry, *IEEE Trans. Nucl. Sci.* **51**, 91 (2004)
4. M. Toyoda, K. Araki, Y. Suzuki, *Opt. Eng.* **41**, 145 (2002)
5. L. Zhang, Y. Yang, W. Xia, X. Zhu, W. Chen, Y. Lu, *Chin. Opt. Lett.* **7**, 728 (2009)
6. M.E. Casey, C. Reynolds, D.M. Binkley, J.M. Rochelle, *Nucl. Inst. Meth. A* **504**, 143 (2003)
7. C.M.B. Monteiro, L.M.P. Fernandes, J.A.M. Lopes, J.F.C.A. Veloso, J.M.F. dos Santos, *Appl. Phys. B* **81**, 531 (2005)
8. G. Binnig, C.F. Quate, C. Gerber, *Phys. Rev. Lett.* **56**, 930 (1986)
9. T.E. Schäffer, J.P. Cleveland, F. Ohnesorge, D.A. Walters, P.K. Hansma, *J. Appl. Phys.* **80**, 3622 (1996)
10. M. Reinstaedtler, U. Rabe, V. Scherer, J.A. Turner, W. Arnold, *Surf. Sci.* **532**, 1152 (2003)
11. C. Yang, A. Bossche, P. J. French, K. B. Gavan, H. S. J. van der Zant, H. Sadeghian, J. F. L. Goosen, F. van Keulen, E. W. J. M. van der Drift *IEEE Conf. Sensors*, **869** (2009)
12. J.P. Cleveland, S. Manne, D. Bocek, P.K. Hansma, *Rev. Sci. Instrum.* **64**, 403 (1993)
13. O. Basarir, S. Bramhavar, G. Basilio-Sanchez, T. Morse, K.L. Ekinci, *Opt. Lett.* **35**, 1792 (2010)
14. R. Berger, Ch. Gerber, J.K. Gimzewski, E. Meyer, H.J. Güntherodt, *Appl. Phys. Lett.* **69**, 40 (1996)
15. J.K. Gimzewski, Ch. Gerber, E. Meyer, R.R. Schlittler, *Chem. Phys. Lett.* **217**, 589 (1994)
16. J. Varesi, J. Lai, T. Perazzo, Z. Shi, A. Majumdar, *Appl. Phys. Lett.* **71**, 306 (1997)
17. J.R. Barnes, R.J. Stephenson, C.N. Woodburn, S.J. O'Shea, M.E. Welland, T. Rayment, J.K. Gimzewski, Ch. Gerber, *Rev. Sci. Instrum.* **65**, 3793 (1994)
18. L.M. Manojlović, *Appl. Opt.* **50**, 3461 (2011)
19. Radiation Monitoring Devices (RMD), 44 Hunt Street, Watertown, MA 02472, USA